



Refining a numerical model for device-induced thrombosis and investigating the effects of non-Newtonian blood models

Ling Yang^a, Nicolas Tobin^a, Keefe B. Manning^{a,b,*}

^a Department of Biomedical Engineering, The Pennsylvania State University, University Park, PA, USA

^b Department of Surgery, Penn State Hershey Medical Center, Hershey, PA, USA



ARTICLE INFO

Article history:

Accepted 3 March 2021

Keywords:

Cardiovascular

Devices

Thrombosis

Computational fluid dynamics

Non-Newtonian

ABSTRACT

Thrombosis is one of the main causes of failure in device implantation. Computational thrombosis simulation is a convenient approach to evaluate the risk of thrombosis for a device. However, thrombosis is a complicated process involving multiple species and reactions. Application of a macroscopic, single-scale computational model for device-induced thrombosis is a cost-effective approach. The current study has refined an existing thrombosis model, which simulated thrombosis by tracing four species in blood: non-activated platelets, activated platelets, surface adherent platelets, and ADP. Platelets are activated mechanically by shear stress, and chemically by ADP. Platelet adhesion occurs on surfaces with low wall shear stress with platelet aggregation inhibited in regions of high shear stress. The study improves the existing thrombosis model by: 1) Modifying the chemical platelet activation function so that ADP activates platelets; 2) Modifying the function describing thrombus deposition and growth to distinguish between thrombus deposition on wall surfaces and thrombus growth on existing thrombus surfaces; 3) Modifying the thrombus breakdown function to allow for thrombus breakdown by shear stress; 4) Modeling blood flow as non-Newtonian. The results show that the inclusion of ADP and the use of a non-Newtonian model improve agreement with experimental data.

© 2021 Elsevier Ltd. All rights reserved.

1. Introduction

Hemostasis is a normal and necessary process in the human body, which prevents blood loss upon injury by sealing the endothelium. However thrombosis, or clots forming in the wrong place, can lead to lethal situations, such as strokes and heart attacks due to vessel occlusion. While thrombosis can occur naturally, it is also a major risk factor for implanted blood-contacting devices. While tissue injury initiates the extrinsic coagulation cascade, blood contact with a foreign surface leads to the intrinsic coagulation cascade, initiated by contact activation of factor XII (Vogler and Siedlecki, 2009). Both pathways activate thrombin, which converts fibrinogen into fibrin. The cross-linked fibrin forms a thrombus. Based on Virchow's triad, device-induced thrombosis oftentimes results from interaction between blood, a surface, and interrupted flow, such as that due to irregular geometry, which induces an abnormal shear distribution within blood flow (Chung and Lip, 2003). Most platelets in the circulation are not activated. When they experience a sufficient shear stress or biochemical

factor, they become activated and tend to aggregate in regions of low wall shear stresses. The activated platelets release platelet agonists and produce additional chemical factors that trigger the coagulation cascade (Gorbet and Sefton, 2004; Navitsky et al., 2013; Stegner and Nieswandt, 2011).

The increasing knowledge of thrombosis and enhanced computational power make numerical simulation of thrombosis possible and a useful tool for evaluating the effects of hemodynamics and biochemical factors on thrombosis. The main challenge of computational simulations is that thrombosis is a multi-scale process involving multiple reactions (De Biasi et al., 2015; Saba and Roberts, 2014; Uriel et al., 2014). While blood flow happens at macroscopic scales in space and time, the biochemical reactions and linking of fibrin occur at much smaller scales ranging from nanometers to micrometers. For example, an aorta (centimeters in diameter) has red blood cells passing through for days while platelets (micrometers in diameter) can be activated within a second. In addition, as more than 80 reactions are involved in thrombosis (Cito et al., 2013), it is computationally expensive to consider all thrombotic reactions in numerical simulations. To reduce the complications due to scales and biochemical reactions, applying a macroscopic thrombosis model that simulates thrombosis at a

* Corresponding author at: The Pennsylvania State University, Department of Biomedical Engineering, 122 CBE Building, University Park, PA 16802, USA.

E-mail address: kbm10@psu.edu (K.B. Manning).

single-scale in space and time and with a reduced-order model of the biochemistry is a convenient approach. Numerical studies have shown that single-scale models can provide accurate predictions in thrombosis (Fogelson and Guy, 2008; Goodman et al., 2005; Menichini and Xu, 2016; Sorensen et al., 1999; Taylor et al., 2016). This type of modeling typically assumes the region of interest to be a continuum in which the biochemical species are characterized through the convection-diffusion-reaction equations and the fluid flow through the Navier-Stokes equations.

Taylor et al. developed a macroscopic thrombosis model based on experimental data, which simulated thrombus growth with non-activated platelets, activated platelets, and ADP (Taylor et al., 2016). While this model can simulate thrombus deposition and growth, it has limitations: (1) The model was applied for two-dimensional simulations where the three-dimensional effects were ignored. (2) The model assumed the rate of chemical platelet activation by ADP to increased indefinitely with the ADP concentrations, which does not match the experimental observations whereby a saturating effect occurred (Chatterjee et al., 2010; Frojmovic et al., 1994). (3) Though the model included the thrombus breakdown mechanism, it was never activated, and (4) the model did not distinguish the process of thrombus deposition on walls from the process of thrombus growth.

To describe the device-induced thrombosis procedure, the current study proposes to modify the computational thrombosis model developed by Taylor et al. (2016), address the aforementioned limitations, and perform three-dimensional (3D) simulations to provide predictions on thrombus deposition and growth in a time scale relevant to medical devices. The objective is to develop a computational model that better describes the 3D macroscopic device-induced thrombosis behavior.

2. Methods

2.1. Computational model

To predict thrombus deposition and growth at the macroscopic scales in space and time, a modified version of the thrombosis model developed by Taylor et al. was used (Taylor et al., 2016). The modifications included alternative reaction rates for platelet activation by ADP, thrombus growth due to platelet-platelet interactions, and thrombus breakdown by shear stress. Details of the computational model are available in the [Supplementary Material](#).

2.2. Numerical simulations

Numerical simulations were performed using an open-source computational fluid dynamics package, OpenFOAM (OpenCFD, Ltd, Bracknell, UK). The finite-volume method was applied with the velocity and pressure fields solved by the pressure implicit with splitting of operator (PISO) algorithm. When thrombosis occurred, the model was coupled with the PISO algorithm so that the velocity and pressure fields were influenced by the presence of the thrombus.

2.2.1. Computational domain

A 3D sudden expansion was used, which was equivalent to the backward facing step (BFS) device used by Taylor et al. whose data were used as foundation and validation for the thrombosis model developed in the current study (Taylor et al., 2014). As shown in [Fig. 1](#), flow entered from the inlet (7.5 mm in height) and exited at the outlet (10 mm in height). The upstream section was 200 mm long, and the downstream section was 100 mm long. Presence of the step (2.5 mm in height) resulted in flow recirculation

and induced thrombosis, as observed by Taylor et al. (2014) and Yang et al. (2020).

2.2.2. Computational details

The no-slip velocity condition was imposed at all wall boundaries, with a fixed velocity at the inlet, and a zero-gradient boundary condition for the velocity outlet. The pressure was set to zero at the outlet, and a zero-gradient boundary condition was used at all other boundaries. For some simulations, the blood flow was assumed Newtonian and steady. The kinematic viscosity for the Newtonian simulations was 3.5 cSt, the asymptotic value of whole bovine blood measured by Taylor et al. (2014) and Yang et al. (2020). The mean velocity at the inlet was set to be 0.201 m/s so that the Reynolds number ($Re = 490$) matched that of both MRI studies. The initial species concentrations involved in the thrombosis model were all set to zero except for platelets. The initial total platelet concentration in bovine blood was estimated as 500×10^6 platelets/mL according to Soloviev et al. (1999). Assuming 5% background platelet activation, the initial activated platelet concentration was 25×10^6 platelets/mL, leaving 475×10^6 platelets/mL of non-activated platelets.

Time differencing was done with a Crank Nicolson scheme. Convection of passive scalars used first-order upwind differencing, while convection of momentum used a second-order upwind scheme. Diffusion terms used second-order differencing. Reaction terms were explicit.

2.2.3. Thrombosis simulations

To mimic the starting flow condition in the MRI experiment, where flow was zero, the current study set the velocity field to be zero initially, when the thrombosis model was initiated. Thrombosis in the BFS model was simulated for 30 min. The resultant aggregation intensity (ε in Equation (1)) and thrombus index (TI in Equation (2)) were used to quantify thrombus formation. Equation (1) is the evolution equation for the aggregation intensity, and depends on the concentration of activated platelets (ϕ_a), a local thrombus susceptibility potential depending on the local shear stress (P_{TSP}), an embolization function, which also depends on the local shear stress (β_e), and fitted constants α_e and B. In Equation (1), the first term allows the aggregation intensity to grow in areas with high concentration of activated platelets, and the second term embolizes adhered platelets in the presence of high shear. Equation (2) defines TI as a thrombus identification parameter locally normalized by total platelet concentration, where ϕ_n is the concentration of non-activated platelets. Additional details of the equations are available in the [Supplementary Material](#). Metrics of the simulated thrombus including height, length, volume, and surface area exposed to blood flow, were calculated based on the geometry of the computational cells which contained ε or TI values greater than their threshold values. The height is reported as the maximum cell-center height where the thresholds are exceeded, with the length being the maximum distance in the streamwise direction where the thresholds are exceeded. Reported volumes are the sum of the volumes of computational cells which exceed thresholds, and surface area is the sum of the areas of cell faces on threshold-exceeding cells that do not face a wall or another thrombus cell. These statistics were computed at different time points and compared to the MRI data in Taylor et al. (2014) and Yang et al. (2020). In addition, the predicted distributions of different blood species were investigated.

$$\frac{d\varepsilon}{dt} = \alpha_e P_{TSP} \phi_a^2 - B \beta_e \varepsilon \quad (1)$$

$$TI = \frac{\varepsilon}{\phi_a + \phi_n} \quad (2)$$

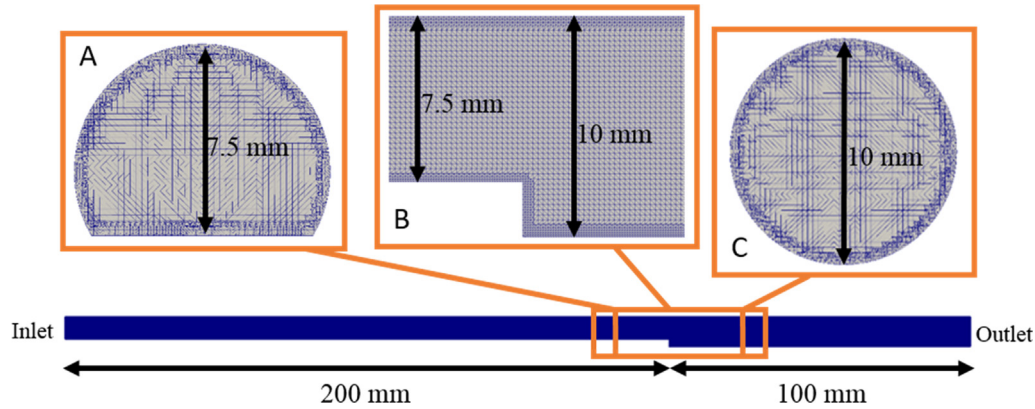


Fig. 1. The three-dimensional BFS model used for computational studies. The dimensions match those of the device used in Taylor et al. (2014) and Yang et al. (2020). The bottom image indicates the centerline plane of the BFS model, with the enlarged step region shown at the top (B). The transverse cross sections of the upstream and downstream are shown (A) and (C), respectively.

2.2.4. Non-Newtonian simulations

Non-Newtonian simulations were performed to investigate the effect of viscosity model on thrombosis predictions. Experiments were done to measure the kinematic viscosity at shear rates ranging from 0.1 to 1000 s^{-1} , and both Carreau (Equation (3)) and cross-power (Equation (4)) viscosity models were fit to the experimental data. Experimental details are described in the Supplement. The initial and boundary conditions remained the same as those for the Newtonian simulations.

$$v = v_{\infty} + (v_0 - v_{\infty}) \left[1 + (k\dot{\gamma})^2 \right]^{\frac{n-1}{2}} \quad (3)$$

$$v = v_{\infty} + \frac{(v_0 - v_{\infty})}{1 + (m\dot{\gamma})^j} \quad (4)$$

2.3. Statistical evaluation of increasingly complex models

The most basic model considered is Newtonian, with no chemical platelet activation, using the aggregation intensity to identify regions of thrombosis. On top of this basic model, we add degrees of freedom constituting chemical platelet activation, quantification by thrombus index, and non-Newtonian flow. The modeling value added by each of these degrees of freedom is evaluated by an F-test using the experimental statistics. Because Taylor et al. (2014) and Yang et al. (2020) report substantially different experimental data, model fits are evaluated based on both sets of data, and p-values are reported to evaluate whether the additional modeling complexity significantly improves agreement with data.

3. Results

The current section focuses on the effects of increasingly complex models. The non-Newtonian model without chemical platelet activation is considered as the base, and additional modeling steps are added to this approach, each with its own subsection. Additional observations are made, including distributions of different species as listed in the [Supplementary Material](#). The three basic velocity fields are presented in the Supplement.

3.1. Addition of ADP modeling

Thrombosis simulations with and without ADP were performed with results appearing in Fig. 2. The solid lines represent thrombosis quantification by the aggregation intensity (grey for the simulation without ADP, and purple for that with ADP). Overlap of the

solid lines during the first 5 min for all metrics suggested that the initial thrombus deposition and growth did not depend on chemical platelet activation by ADP. After 5 min, ADP promoted thrombus growth and sizes of the thrombus continued to increase from 5 to 15 min. The exposed surface area and volume increased significantly and reached the maximum within the range of the experimental data. After 15 min, the thrombus remained asymptotic, with constant sizes and shape.

Based on the results of an F-test considering all experimental time points and one added degree of freedom, the addition of ADP modeling significantly improved thrombus predictions ($p < 0.05$ for Taylor et al. data, $p < 0.01$ for Yang et al. data). Considering the five-minute time point reported in Yang et al., the addition of ADP modeling did not significantly improve model performance ($p = 0.72$), suggesting ADP did not play a significant role in early thrombus deposition.

3.2. Thrombus index quantification

When the thrombus index was used to quantify thrombosis, the simulation results (dashed line) showed that the initial thrombus growth occurred at 5 min and was rapid from 5 to 10 min. Afterwards, the normalized length and normalized height of the thrombus experienced minimal increase, remaining constant after 15 min. The exposed surface area and volume continued to increase from 10 to 20 min and became relatively constant after 25 min. Compared to thrombosis quantification using the aggregation intensity, using the thrombus index delayed the start time of the initial thrombus growth but gave a closer fit to some of the experimental data.

Compared to the model with ADP, quantification of thrombus by thrombus index did not significantly improve model performance for either data set ($p = 0.25$ for Taylor et al. data, agreement with Yang et al. data made worse).

3.3. Non-Newtonian viscosity models

When blood was assumed to be Newtonian, the kinematic viscosity remained constant throughout the BFS model. When blood was described as non-Newtonian, the kinematic viscosity was high in the region with low shear rate and low in the region with high shear rate. As shown in Fig. 3, application of the Carreau model resulted in high viscosity at the step corner, the reattachment point, and the center of the recirculation region, where shear rates were low. Compared to the Carreau model, the cross-power model led to higher viscosity in the recirculation region.

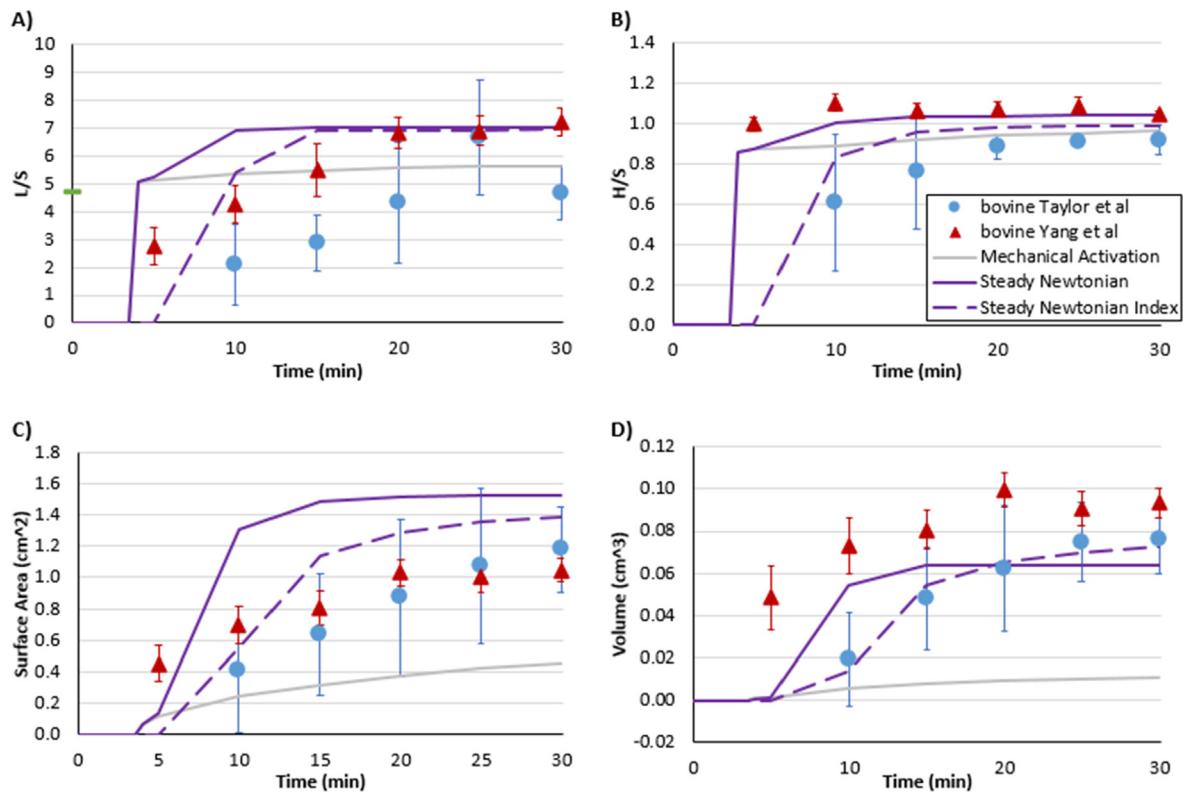


Fig. 2. Thrombosis simulation results (line curves) in comparison to the MRI experimental data provided by Taylor et al. (2014) (blue circle) and Yang et al. (2020) (red triangle) (Taylor et al., 2014; Yang et al., 2020). The MRI data points are the mean values and the error bars represent the SEM. The grey line indicates the simulation where platelets were activated mechanically. The purple lines indicate the simulations where chemical platelet activation by ADP was also involved. The solid line indicates that the thrombus was quantified by the aggregation intensity, while the dashed line indicates quantification by the thrombus index. (A) Normalized length, (B) normalized height, (C) surface area exposed to blood, and (D) volume of the thrombus during 30 min of blood flow are shown. The thrombus length and height were normalized by the step height S (2.5 mm). In (A), the initial centerline reattachment length, normalized by the step height, is shown by the green bar. (For interpretation of the references to color in this figure legend, the reader is referred to the web version of this article.)

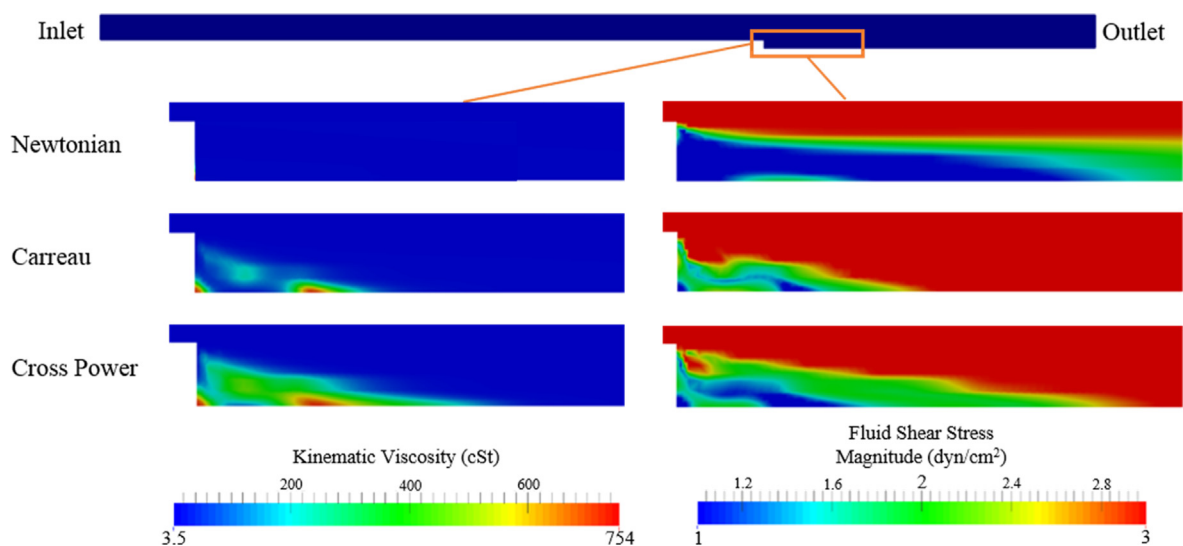


Fig. 3. Initial distribution of the kinematic viscosity and the magnitude of the fluid shear stress along the centerline plane of the BFS model under fully-developed steady flow, with focus on the step region. Blood was assumed to be Newtonian or non-Newtonian, through the Carreau or Cross-Power models.

Distribution of the fluid shear stress (τ_f) is shown in Fig. 3. When flow was steady and blood was assumed to be Newtonian, the fluid shear stress remained low along the region downstream of the step, which promoted thrombus deposition and growth. As a result, a large thrombus was obtained by 30 min (Fig. 4, Newtonian). When blood was assumed to be non-Newtonian, the region

with low fluid shear stress was restricted and became shorter in length. However, at the step corner and the reattachment point, the fluid shear stress remained low, promoting growth in aggregation intensity. Values in these regions were less than 1 dyn/cm², the threshold value below which the thrombus susceptibility potential P_{TSP} (Equation (14) in the Supplementary Material)

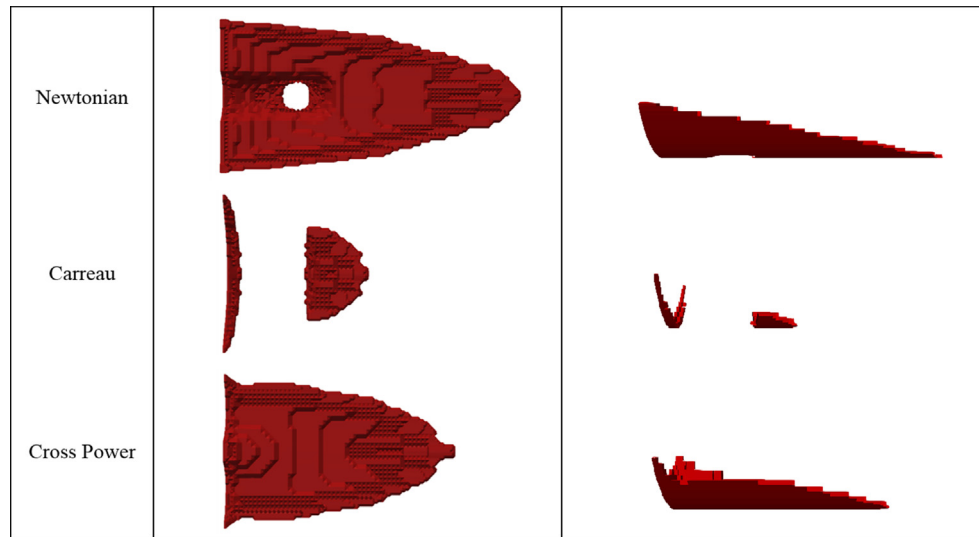


Fig. 4. Simulated thrombi at 30 min of blood flow resulted from different simulations. Inlet flow was steady. Blood was assumed to be Newtonian or non-Newtonian, through the Carreau or Cross-Power models. Top views are on the left, and side views are on the right.

reached the maximum (*i.e.* 1) (Taylor et al., 2016) and allowed thrombus to form unimpeded. Consequently, the Carreau simulation predicted small thrombus formation at the step and the reattachment point, with shorter total length (Fig. 4, Carreau). Compared to the Carreau simulation, the Cross-Power simulation resulted in a larger low shear stress region at the step and the fluid shear stress was lower at the center of flow recirculation, which promoted thrombus growth within the recirculation. By 30 min of blood flow, a longer thrombus was generated, with a filled center (Fig. 4, Cross-Power).

Because thrombus quantification by thrombus index did not significantly improve agreement with data, aggregation intensity was used to quantify thrombi in non-Newtonian simulations. The results are shown in Fig. 5, in comparison to those from the Newtonian simulation. With the non-Newtonian models, the thrombus started to grow at 4 min. Thrombus size increased rapidly from 5 to 10 min due to chemical platelet activation by ADP, which increased the concentration of activated platelets and enhanced platelet aggregation. After 15 min, the thrombus remained asymptotic, with constant sizes.

Compared to the Newtonian simulation, the Carreau simulation (Fig. 5, orange line) predicted a thrombus whose sizes were much smaller, especially the exposed surface area and volume. As shown in Fig. 4, the Carreau simulation resulted in small thrombi aggregated at the step corner and the reattachment point, with a large gap in between. Therefore, the overall thrombus sizes remained small.

When the Cross-Power model was used, the thrombus was smaller than the Newtonian simulation but larger than the Carreau simulation (Fig. 4). In addition to the difference in size, the Cross-Power simulation generated a thrombus whose center was filled, which agreed with the experimental observations (Taylor et al., 2014; Yang et al., 2020). As a result, sizes of the simulated thrombus matched the experimental measurements at early time points, from 0 to 15 min (Fig. 5, pink line). After 15 min, while the thrombus continued to grow in the experiments, the simulated thrombus remained asymptotic and smaller than those from the experiments.

The early length of the simulated thrombus matched the length of the recirculation region. The low shear stress at the step corner and the reattachment point led to platelet aggregation and thrombus formation at these regions. As shown in Fig. 5 (A), the initial

length of the thrombus was approximately the reattachment length (green symbols) for both the Newtonian and non-Newtonian simulations.

Though the Newtonian and non-Newtonian simulations resulted in recirculation regions with similar heights (Fig. 5 (B)), the thrombi had different heights. In the Newtonian simulation, the thrombus reached the height of the recirculation region initially and increased further from 5 to 10 min when ADP was included, and thrombosis was promoted. In the Cross-Power simulation, the thrombus height was lower than that of the recirculation region initially, increased from 5 to 15 min, and remained constant afterwards. The thrombus height reached a maximum similar to the recirculation height. In the Carreau simulation, the trend of increased thrombus height was similar to that from the Cross-Power simulation. However, the Carreau simulations resulted in higher shear stresses within the recirculation region, which restricted platelet aggregation, and the simulated thrombus was smaller, with a lower maximum height.

As compared to the Newtonian model with platelet activation by ADP, the Carreau viscosity model made agreement with experimental data worse. In contrast, the cross-power viscosity model improved agreement with both experimental data sets ($p < 0.01$).

3.4. Chemical and mechanical limiting mechanisms

As shown in Fig. 6, during the first 5 min, the ADP concentration was below the threshold (*i.e.* the normalized ADP was below 1), and chemical platelet activation was minimal. Only the mechanical effects were involved, leading to overlap between the grey and purple solid lines in Fig. 2. Thrombi aggregated at the corner and the reattachment point, resulting in small thrombi. The ADP concentration continued to increase and exceeded the threshold after 5 min (Fig. 6). As a result, platelets were activated chemically, which led to significant increase in activation, and growth dominated by ADP. From 5 to 15 min, the exposed surface area increased 12 times, and the volume increased 6-fold. After 15 min, the ADP concentration was at least 10 times greater than the threshold. According to Equation (8) in the [Supplementary Material](#), with high ADP concentration, A_c reached the maximum (*i.e.* k_{ADP}) and remained constant. There was no further increase in platelet activation, and the simulated thrombus was asymptotic due to an equilibrium between the growth and decay terms in the

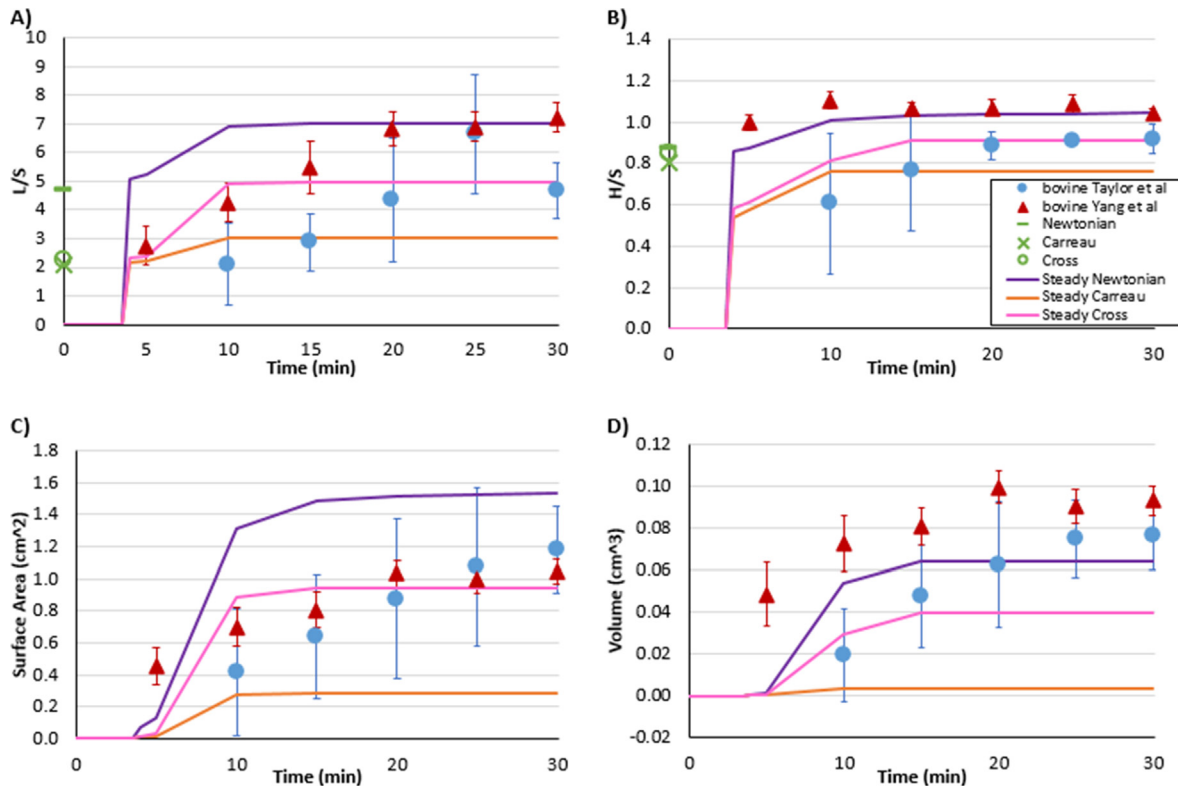


Fig. 5. Thrombosis simulation results (line curves) in comparison to the MRI experimental data provided by Taylor et al. (2014) (blue circle) and Yang et al. (2020) (red triangle) (Taylor et al., 2014; Yang et al., 2020). The MRI data points are the mean values and the error bars represent the SEM. Flow is steady for all simulations. Thrombus is quantified by the aggregation intensity. Purple line indicates the Newtonian simulation. Orange line indicates simulation applying the Carreau model and pink line for the Cross-Power model. (A) Normalized length, (B) normalized height, (C) surface area exposed to blood, and (D) volume of the thrombus during 30 min of blood flow are shown. The thrombus length and height are normalized by the step height (2.5 mm). In (A) and (B), green symbols indicate the initial length and height of the recirculation region for Newtonian and non-Newtonian simulations. (For interpretation of the references to color in this figure legend, the reader is referred to the web version of this article.)

evolution equation for aggregation intensity (Supplementary Material, Equation (11)). The decay term β is a function of the scalar shear stress, and primarily acts on the surface of the thrombus where shear is highest. A similar phenomenon has previously been observed, in which the simulated thrombus became asymptotic when platelet activation by ADP, thrombin, and other coagulants was limited (Leiderman and Fogelson, 2013).

Because there was no inhibitory mechanism for production of ADP, the concentration of ADP continued to increase over time (Fig. 6). The current thrombosis model could be improved by incorporating ADP consumption slowing thrombus growth.

4. Discussion

The current section focuses on comparisons between simulation results and experimental data, and the effects of non-Newtonian blood behavior on thrombosis with additional information and model limitations available in the Supplementary Material.

4.1. Comparison of growth behavior to experimental data

The Newtonian simulations predicted that asymptotic thrombus shape would be achieved after 20 min, which agreed with the experimental observations. While MRI experiments showed that the thrombus length increased smoothly at early time points, the simulated thrombus achieved the asymptotic length in 15 min, due to thrombus deposition at the reattachment point which was not seen in the experiments. As a result, the predicted thrombus length disagreed with the experimental data at early time points.

However, all asymptotic thrombus lengths were similar to the experimental data.

When thrombosis was quantified by the aggregation intensity (Fig. 2), the length, height, and exposed surface area of the simulated thrombus agreed with the bovine experimental measurements (Yang et al., 2020). However, the volume of the simulated thrombus was low due to the hollow center (Fig. 4, Newtonian), which was not observed during the experiments. This gap in the simulations occurred because wall shear stress was high enough at the center of the recirculation region to prevent thrombus growth.

4.2. Effects of Non-Newtonian blood behavior

For the current study, to determine the effects of non-Newtonian blood behavior, the Carreau and Cross-Power models were implemented individually due to their common applications and ability to provide finite viscosity values at low shear rates (Chen and Lu, 2006; Johnston et al., 2004; Marrero et al., 2014; Molla and Paul, 2012; Soulis et al., 2008).

For the Carreau simulation, shear stress was high within the recirculation region except at the step corner and the reattachment point, which restricted thrombus deposition and growth in these regions. By 30 min, small thrombi had formed at the step corner and the reattachment point (Fig. 4, Carreau), with sizes much smaller than the Newtonian simulation, and disagreed with the experimental measurements (Fig. 5, orange line).

Shear stress was lower within the recirculation region (Fig. 3) with the cross-power model than with the Carreau model, which promoted platelet aggregation and thrombosis. By 30 min, a larger

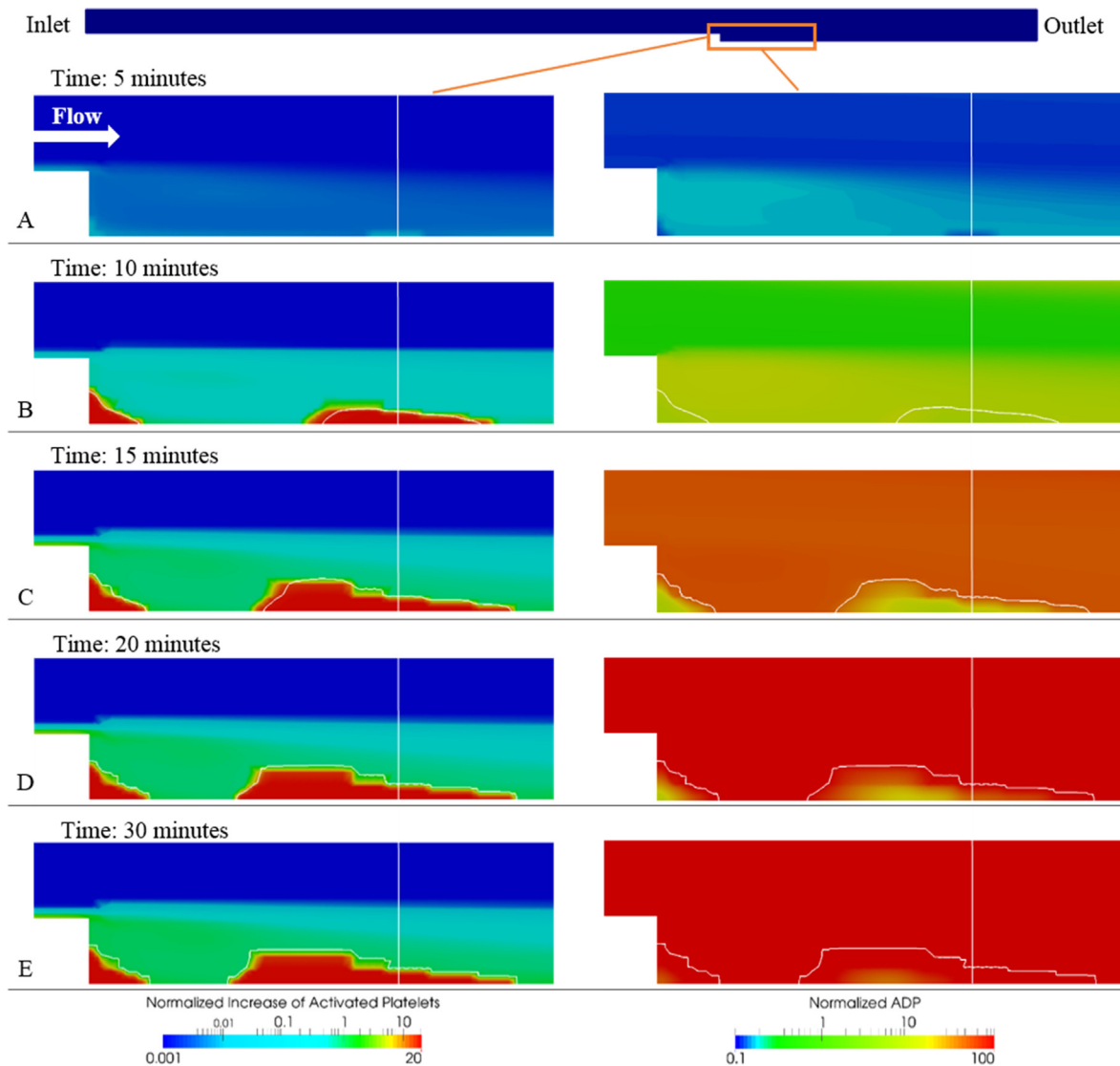


Fig. 6. Distribution of the normalized increase of activated platelets $[(\phi_a - \phi_{a,initial})/\phi_{a,initial}]$ and the normalized ADP (ADP/ADP_t) along the centerline plane of the BFS model from 5 to 30 min, with focus on the step region. Flow is steady and Newtonian. In the color maps, surfaces of the simulated thrombi are highlighted by the white curves, while location of the reattachment point is indicated by the white vertical line. Logarithmic scales are applied.

thrombus had formed with a filled center (Fig. 4, Cross-Power), which agreed with the experiments (Taylor et al., 2014; Yang et al., 2020). The filled thrombus structure allowed the thrombus sizes to match the experimental measurements at early time points (Fig. 5, pink line), from 5 to 15 min. Unlike the experiments, the thrombus did not continue to grow after 15 min and ended up producing a thrombus smaller than the experiments.

4.3. Conclusions

The current study refined a previously developed thrombosis model with improvements including 3D simulation, ADP-induced platelet activation, thrombus breakdown, and non-Newtonian viscosity models. Results showed that inclusion of ADP-induced platelet activation and a cross-power non-Newtonian model led to significant improvement in model predictions, while quantification with thrombus index did not. While shear-induced platelet activation led to initial deposition, ADP-induced platelet activation dominated thrombus growth. Non-Newtonian blood behavior

restricted thrombosis but led to better agreement with experimental data.

In attempting to better match the experimental thrombosis results, we have added some complexity to better match the true processes leading to thrombosis. There are, however, still significant assumptions and simplifications such as the lack of thrombin or fibrin modeling. The biochemistry used in the model does not represent the true complexity of reactions that occur in the blood. Recent work (Link et al. 2020) has gone into more faithfully representing the coagulation cascade, an approach that may lead to better thrombosis predictions. The ability of the model to predict thrombosis in other geometries and flow conditions also remains to be tested.

Declaration of Competing Interest

The authors declare that they have no known competing financial interests or personal relationships that could have appeared to influence the work reported in this paper.

Acknowledgments

This research was supported, in part, by NIH Grant T32GM108563 and HL136369. NIH did not have any involvement in the study design, in the collection, analysis and interpretation of data; in the writing of the manuscript; and in the decision to submit the manuscript for publication.

Appendix A. Supplementary material

Supplementary data to this article can be found online at <https://doi.org/10.1016/j.jbiomech.2021.110393>.

References

- Chatterjee, M.S., Purvis, J.E., Brass, L.F., Diamond, S.L., 2010. Pairwise agonist scanning predicts cellular signaling responses to combinatorial stimuli. *Nat. Biotechnol.* 28, 727–732. <https://doi.org/10.1038/nbt.1642>.
- Chen, J., Lu, X.Y., 2006. Numerical investigation of the non-Newtonian pulsatile blood flow in a bifurcation model with a non-planar branch. *J. Biomech.* 39, 818–832. <https://doi.org/10.1016/j.jbiomech.2005.02.003>.
- Chung, I., Lip, G.Y.H., 2003. Virchow's triad revisited: Blood constituents. *Pathophysiol. Haemost. Thromb.*, 449–454. <https://doi.org/10.1159/000083844>.
- Cito, S., Mazzeo, M.D., Badimon, L., 2013. A review of macroscopic thrombus modeling methods. *Thromb. Res.* <https://doi.org/10.1016/j.thromres.2012.11.020>.
- De Biasi, A.R., Manning, K.B., Salemi, A., 2015. Science for surgeons: Understanding pump thrombogenesis in continuous-flow left ventricular assist devices. *J. Thorac. Cardiovasc. Surg.* 149, 667–673. <https://doi.org/10.1016/j.jtcvs.2014.11.041>.
- Fogelson, A.L., Guy, R.D., 2008. Immersed-boundary-type models of intravascular platelet aggregation. *Comput. Methods Appl. Mech. Eng.* 197, 2087–2104. <https://doi.org/10.1016/j.cma.2007.06.030>.
- Frojmovic, M.M., Mooney, R.F., Wong, T., 1994. Dynamics of platelet glycoprotein IIb-IIIa receptor expression and fibrinogen binding. I. Quantal activation of platelet subpopulations varies with adenosine diphosphate concentration. *Biophys. J.* 67, 2060–2068. [https://doi.org/10.1016/S0006-3495\(94\)80689-7](https://doi.org/10.1016/S0006-3495(94)80689-7).
- Goodman, P.D., Barlow, E.T., Crapo, P.M., Mohammad, S.F., Solen, K.A., 2005. Computational model of device-induced thrombosis and thromboembolism. *Ann. Biomed. Eng.* 33, 780–797. <https://doi.org/10.1007/s10439-005-2951-z>.
- Gorbet, M.B., Sefton, M.V., 2004. Biomaterial-associated thrombosis: Roles of coagulation factors, complement, platelets and leukocytes. *Biomaterials.* <https://doi.org/10.1016/j.biomaterials.2004.01.023>.
- Johnston, B.M., Johnston, P.R., Corney, S., Kilpatrick, D., 2004. Non-Newtonian blood flow in human right coronary arteries: Steady state simulations. *J. Biomech.* 37, 709–720. <https://doi.org/10.1016/j.jbiomech.2003.09.016>.
- Leiderman, K., Fogelson, A.L., 2013. The Influence of Hindered Transport on the Development of Platelet Thrombi Under Flow. *Bull. Math. Biol.* 75, 1255–1283. <https://doi.org/10.1007/s11538-012-9784-3>.
- Link, K.G., Stobb, M.T., Sorrells, M.G., Bortot, M., Ruegg, K., Manco-Johnson, M.J., Di Paola, J.A., Sindi, S.S., Fogelson, A.L., Leiderman, K., Neeves, K.B., 2020. A mathematical model of coagulation under flow identifies factor V as a modifier of thrombin generation in hemophilia A. *J. Thromb. Haemost.* 18, 306–317.
- Marrero, V.L., Tichy, J.A., Sahni, O., Jansen, K.E., 2014. Numerical study of purely viscous non-newtonian flow in an abdominal aortic aneurysm. *J. Biomech. Eng.* 136. <https://doi.org/10.1115/1.4027488>.
- Menichini, C., Xu, X.Y., 2016. Mathematical modeling of thrombus formation in idealized models of aortic dissection: initial findings and potential applications. *J. Math. Biol.* 73, 1205–1226. <https://doi.org/10.1007/s00285-016-0986-4>.
- Molla, M.M., Paul, M.C., 2012. LES of non-Newtonian physiological blood flow in a model of arterial stenosis. *Med. Eng. Phys.* 34, 1079–1087. <https://doi.org/10.1016/j.medengphy.2011.11.013>.
- Navitsky, M.A., Deutsch, S., Manning, K.B., 2013. A thrombus susceptibility comparison of two pulsatile penn state 50 cc left ventricular assist device designs. *Ann. Biomed. Eng.* 41, 4–16. <https://doi.org/10.1007/s10439-012-0627-z>.
- Saba, H.L., Roberts, H.R. (Eds.), 2014. Hemostasis and Thrombosis: Practical Guidelines in Clinical Management. John Wiley & Sons, Ltd, Oxford, UK. <https://doi.org/10.1002/9781118833391>.
- Soloviev, M.V., Okazaki, Y., Harasaki, H., 1999. Whole blood platelet aggregation in humans and animals: A comparative study. *J. Surg. Res.* 82, 180–187. <https://doi.org/10.1006/jsre.1998.5543>.
- Sorensen, E.N., Burgreen, G.W., Wagner, W.R., Antaki, J.F., 1999. Computational Simulation of Platelet Deposition and Activation: I. Model Development and Properties. *Ann. Biomed. Eng.* 27, 436–448. <https://doi.org/10.1114/1.200>.
- Soulis, J.V., Giannoglou, G.D., Chatzizisis, Y.S., Seralidou, K.V., Parcharidis, G.E., Louridas, G.E., 2008. Non-Newtonian models for molecular viscosity and wall shear stress in a 3D reconstructed human left coronary artery. *Med. Eng. Phys.* 30, 9–19. <https://doi.org/10.1016/j.medengphy.2007.02.001>.
- Stegner, D., Nieswandt, B., 2011. Platelet receptor signaling in thrombus formation. *J. Mol. Med.* <https://doi.org/10.1007/s00109-010-0691-5>.
- Taylor, J.O., Meyer, R.S., Deutsch, S., Manning, K.B., 2016. Development of a computational model for macroscopic predictions of device-induced thrombosis. *Biomech. Model. Mechanobiol.* 15, 1713–1731. <https://doi.org/10.1007/s10237-016-0793-2>.
- Taylor, J.O., Witmer, K.P., Neuberger, T., Craven, B.A., Meyer, R.S., Deutsch, S., Manning, K.B., 2014. In vitro quantification of time dependent thrombus size using magnetic resonance imaging and computational simulations of thrombus surface shear stresses. *J. Biomech. Eng.* 136. <https://doi.org/10.1115/1.4027613>.
- Uriel, N., Han, J., Morrison, K.A., Nahumi, N., Yuzefpolskaya, M., Garan, A.R., Duong, J., Colombo, P.C., Takayama, H., Thomas, S., Naka, Y., Jorde, U.P., 2014. Device thrombosis in HeartMate II continuous-flow left ventricular assist devices: A multifactorial phenomenon. *J. Hear. Lung Transplant.* 33, 51–59. <https://doi.org/10.1016/j.healun.2013.10.005>.
- Vogler, E.A., Siedlecki, C.A., 2009. Contact activation of blood-plasma coagulation. *Biomaterials* 30, 1857–1869. <https://doi.org/10.1016/j.biomaterials.2008.12.041>.
- Yang, L., Neuberger, T., Manning, K.B., 2020. In vitro real-time magnetic resonance imaging for quantification of thrombosis. *Magn. Reson. Mater. Phys. Biol. Med.* 1–11. <https://doi.org/10.1007/s10334-020-00872-2>.